Molecular Rotors as Reactivity Probes: Predicting Electrophilicity from the Speed of Rotation

Hao Liu,[a] Xiaolong Huang,[a] Binzhou Lin,[a] Harrison M. Scott,[a] Ishwor Karki,[a] Erik C. Vik,[a] Perry J. Pellechia,[a] and Ken D. Shimizu*[a]

[a] Dr. H. Liu, Xiaolong Huang, Dr. Binzhou Lin, Harrison M. Scott, Dr. Ishwor Karki, Dr. Erik C. Vik, Dr. Perry J. Pellechia, and Prof. K. D. Shimizu
Department of Chemistry and Biochemistry
University of South Carolina
Columbia, SC 29205
E-mail: shimizu@mailbox.sc.edu

Supporting information for this article is given via a link at the end of the document

Abstract: A new empirical electrophilicity reactivity parameter, E_{RB}, was developed based on the rotational barriers of a series of *N*-phenylimide molecular rotors containing various electrophilic groups. In the bond rotation transition state, these electrophilic groups form close contact with an electronegative C=O oxygen. Thus, strong electrophilic groups significantly lowered the rotational barrier. As a result, the rotational barriers were inversely correlated with the strengths of the electrophiles. The rotational barriers were measured by dynamic NMR (EXSY), enabling the quantification across a wide range of types of electrophiles. Computational analysis confirmed that the observed variations arose from intramolecular interactions in the transition state, where the C=O oxygen served as a probe of both the electrophilic group's electrostatic potential and steric accessibility. By simultaneously capturing attractive and repulsive transition state interactions, E_{RB} provides an effective means of predicting electrophilicity and reactivity trends across a broad range of electrophiles and reaction types. The utility of E_{RB} was initially validated using a series of rotors containing Michael addition electrophiles, followed by broader application to a diverse array of reactions involving sp^3 and sp^2 electrophiles, including S_N2, S_NAr, Pd-oxidative addition, and Sonogashira reactions.

INTRODUCTION

Electrophilicity trends play a crucial role in predicting reaction outcomes in organic synthesis, optimizing lead compounds in drug discovery, and tuning electronic properties in materials design.[1–6] Electrophile reactivity scales and parameters are useful in predicting reactivity trends, providing insight into reaction mechanisms, and serving as benchmarks to improve the accuracy of computational models.[7] However, existing electrophilicity parameters typically capture either attractive electrostatic and orbital effects or repulsive steric effects, but rarely both. In this report, we introduce a new empirical electrophilicity parameter, E_{RB}, based on the rotational barriers ($\Delta G^{\ddagger}$) of a series of *N*-phenylsuccinimide molecular rotors (Figure 1a), containing the electrophilic groups. The parameter is easy to measure using dynamic NMR and can be applied to a wide range of electrophiles. This was initially demonstrated by using E_{RB} values obtained from rotor **R1** to predict the electrophilicity of Michael acceptors (Figure 2). Then, the broader utility of E_{RB} was demonstrated by rotors **R2** and **R3** designed to predict electrophilicities in the S_N2, S_NAr, and Sonogashira reactions. These reactions differ significantly in mechanism and in the hybridization of the electrophilic carbon, and they have not been comprehensively analyzed by existing electrophilicity parameters. This underscores E_{RB}'s potential to address limitations in current electrophilicity models and parameters.

The rotors consist of a rotating phenyl unit connected to the nitrogen of a bicyclic succinimide framework, with electrophilic groups integrated at the *ortho*-position of the rotating phenyl ring. In the bond rotation transition state (TS), the electrophilic group forms close contact with an electronegative imide oxygen. These TS interactions share key structural and electronic features with nucleophile–electrophile interactions in bond forming reactions, such as distance and angle of approach (*vide infra*). However, no bond formation occurs, and thus, the rotors are not direct models of bond-forming transition states.

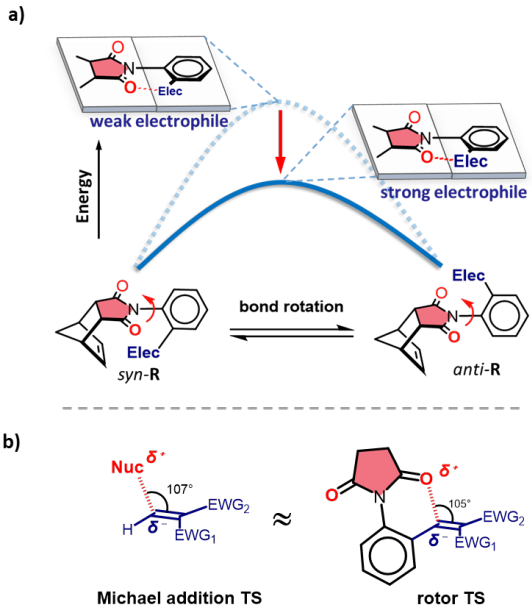

Figure 1. a) Schematic representation of how rotational barriers can serve as a measure of electrophilicity for the attached electrophilic group (Elec). In the *syn-anti* conformational equilibrium of rotors R, strong electrophiles form stronger TS-stabilizing intramolecular interactions, leading to systematically lower rotational barriers. b) Comparison of the structural similarities between the Michael addition reaction TS and the bond rotation TS of a *N*-phenylsuccinimide molecular rotor R1, which contains a Michael acceptor group.

Nevertheless, the geometric and electronic similarities are expected to produce comparable trends in transition state stabilization and reactivity. In this framework, the imide C=O

oxygen effectively serves as a nucleophilic probe for the electrophilicity of the attached group. Stronger electrophiles produce greater stabilization of the transition state, leading to lower rotational barriers. This correlation between rotational barriers and electrophilicity forms the basis for a new empirical electrophilicity parameter, E_{RB}. E_{RB} is defined as the difference in rotational barriers ($\Delta G^{\neq}$) in kcal/mol between a control rotor with the weakest electrophile and a rotor containing the electrophile of interest ($E_{RB} = \Delta G^{\neq}_{control} - \Delta G^{\neq}_{electrophile}$). This order of operations ensures that E_{RB} values are positive and increase with increasing electrophilicity. In this study, the control rotor is **R1i**, which contains an unsubstituted ethylene group and represents the weakest electrophile in the Michael acceptor series. This control was retained across the different electrophile classes and reactions, providing consistency to the E_{RB} values.

The development of reactivity parameters based on model systems has a long history of providing experimentally accessible insights into reaction mechanisms. Although the use of model systems to study and predict the rates and reactivities was a strategy originally developed before the advent of modern computational chemistry, they remain widely utilized in mechanistic and reaction optimization studies. Examples of commonly employed reactivity parameters include Hammett's σ parameter based on the protonation equilibrium of substituted benzoic acids,[8–10] and Lewis acidity scales such as the Gutmann-Beckett method, based on the ^{31}P NMR shift of a specific Lewis base, Et_3PO.[11] Recent applications of these model-based parameters include Jacobson's studies of asymmetric reaction selectivity and Sigman's reactivity predictions based on molecular descriptors.[12–15]

Molecular rotors are well-suited to study reactivity trends due to their ability to detect subtle changes in energy landscapes. They have been used to develop empirical steric parameters that quantify the size of substituents,[16–18] measure the TS stabilizing effects of noncovalent interactions,[19–23] and provide insights into reaction dynamics.[24] Given these capabilities, we hypothesized that molecular rotors would be well-suited for studying nucleophile-electrophile interactions. Molecular rotors offer several benefits in this application. First, rotational barriers are easily measured. Bond rotation is a unimolecular first-order kinetic process, which greatly simplifies measurement and kinetic analysis. By comparison, nucleophile-electrophile reactions are typically bimolecular and have more complex rate equations with multiple reactants to control and monitor.[25–29] Second, the rotational barrier is sensitive to steric and solvent effects, which are absent in the most popular computational electrophilicity parameters such as Parr's local or global ω.[30,31] Third, the rotors can evaluate electrophiles across a wide range of reactivities using a single measurement. By comparison, the empirical electrophilicity parameter E requires measuring the electrophilicity against 3 to 5 nucleophiles to assemble a reactivity ladder.[32–36]

To establish the validity of E_{RB} to assess electrophilicity, we first tested the ability of rotor **R1** (Figure 2) to predict the reactivities of a series of Michael acceptor electrophiles (**E1**). Once the ability of the rotors to predict reactivity trends was established, the broader utility of this approach was tested using rotors **R2** and **R3** to study the S_N2, S_NAr, and Pd-oxidative addition reactions. The corresponding electrophiles, **E2** and **E3**, highlight the versatility of the method, as they represent both sp³ and sp² electrophilic centers and participate in mechanistically distinct reactions. To further evaluate the utility of E_{RB}, we tested whether E_{RB} values generated using DFT calculations of the corresponding rotational barriers could also accurately predict reactivity; this was assessed using a set of aryl halide electrophiles in the Sonogashira reaction.

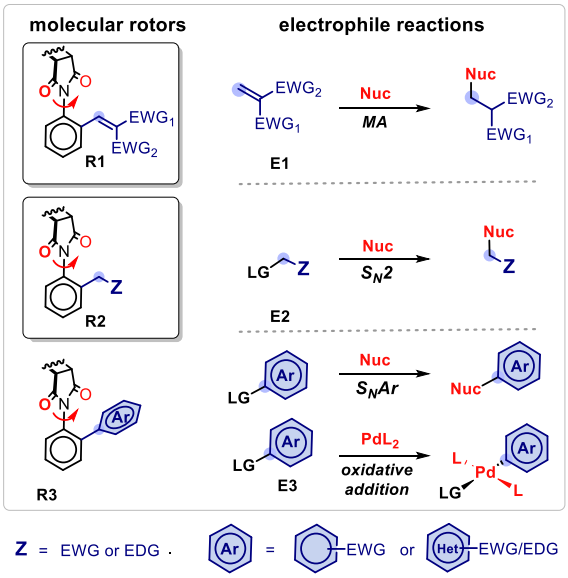

Figure 2. Molecular rotors **R1**, **R2**, and **R3** (left) designed to study electrophiles in Michael addition, S_N2, S_NAr, Pd-oxidative addition, and Sonogashira reactions (right). The blue dot highlights the electrophilic carbon in the reaction and rotor electrophilic groups.

The Michael addition reaction was chosen for this initial study for several reasons. First, experimental reactivity data were available in the literature for a range of Michael acceptors, allowing for direct comparison and evaluation of E_{RB}.[32] Second, the strength of the electrophiles could be systematically tuned by adjusting the number of electron-withdrawing groups (EWGs) to cover a broad range of electrophilicities. This structural flexibility allowed us to design a series of rotors **R1** containing Michael acceptors with zero (**R1i**), one (**R1a-e**), and two (**R1f-h**) EWGs (Figure 3). Third, rotors **R1a-h** containing the Michael acceptor electrophiles could be easily synthesized.[37–41]

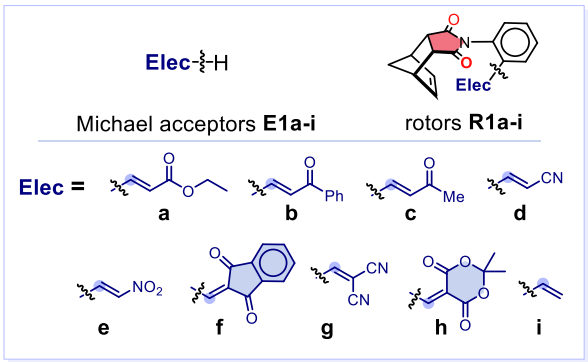

Figure 3. Structures of the *N*-phenylsuccinimide rotors **R1** containing varying Michael acceptors in the *ortho*-position and the corresponding ethylene Michael acceptors electrophiles **E1** used to evaluate E_{RB}. The blue dots highlighted the electrophilic γ-carbon, which has the closest contact to the imide C=O in the bond rotation TS.

RESULTS AND DISCUSSION

Validating the rotor design. To verify that the rotors positioned the imide C=O oxygen and the electrophilic carbon of the *ortho*-R-group in the correct geometry for through-space interaction, we first analyzed the bond rotation transition state structures of rotors **R1a-i** bearing Michael acceptor electrophiles. The DFT-optimized ground state and transition state structures were determined at the B3LYP-D3/6-311G* level of theory, with frequency correction to yield the calculated $\Delta G^{\ddagger}_{298}$. This modest level of theory has previously demonstrated sufficient accuracy in our studies of *N*-phenylsuccinimide and biaryl rotors, as well as in Mazzanti's investigations of similar systems.[16–19,21,22] The accuracy was reconfirmed with the current rotors **R1**–**R3**, as the computed rotational barriers remained within ±0.6 kcal/mol (RMSE) of the experimentally measured values (see SI). In the transition-state structures, the imide oxygen is positioned closest to the γ-carbon of the electrophilic group, which corresponds to the electrophilic carbon of the Michael acceptor (Figure 4a, first structure). The O•••C_γ distances in **R1a-i** were significantly shorter (2.32–2.73 Å) than the sum of the vdW radii of O and C (3.22 Å, Table S1). An example of the TS geometry is shown in Figure 4a for rotor **R1g,** which has an O•••C distance of 2.36 Å. These short distances are indicative of the formation of stabilizing intramolecular electrostatic and orbital-orbital interactions between the imide oxygen and electrophilic carbon (*vide infra*). Equally important, the imide oxygen adopts an orientation similar to that observed in nucleophile-electrophile transition states of Michael addition reactions (Figure 1b). Specifically, the imide oxygen approaches the plane of the Michael acceptor electrophilic groups at an angle of 105°, closely matching the Bürgi–Dunitz angle of 107° for attack on polarized π-bonds.[42]

Rotor synthesis and barrier measurement. Measurement of the E_{RB} value for each electrophile requires a unique molecular rotor, making the synthetic accessibility of the rotors essential. Rotors **R1a-1i** were efficiently prepared in one or two steps by condensing an *ortho*-substituted aniline with *cis*-5-norbornene-*endo*-2,3-dicarboxylic anhydride, with 75% or higher overall yields (See SI).[37–41] The rotors were in conformational equilibrium between *syn*- and *anti*-rotamers (Figure 1a), exhibiting distinct peaks in the NMR spectra below their coalescence temperatures (-20 to 90 °C). This enabled measurement of the rotational barriers ($\Delta G^{\ddagger}$) in TCE-d_2 using variable temperature ^{1}H NMR EXSY with an accuracy of ± 0.2 kcal/mol based on the rate of exchange of the rotamers (Table 1). EXSY is a 2D NMR technique that detects chemical exchange between conformers through cross-peaks in the spectrum. The rotational barriers for rotors **R1a** to **R1i** ranged from 15.5 kcal/mol for **R1h** to 19.8 kcal/mol for **R1i**.

Ease of E_{RB} measurement. These studies also highlighted the ease of measuring E_{RB}, which only requires one rotational barrier measurement. By comparison, Mayr's *E* parameter requires multiple kinetic measurements with 3 to 5 nucleophiles per electrophile. This is necessary as highly reactive nucleophiles react too quickly with strong electrophiles, while weak nucleophiles may not react with less electrophilic substrates. For our approach, the rotors' inability to form a covalent bond in the TS was advantageous, as it enabled the use of a single "nucleophile", the carbonyl oxygen, to probe both weak and strong electrophiles. Moreover, the EXSY NMR method used to measure the rotational barriers offers a wide dynamic range (10 to 24 kcal/mol), sufficient to span the full range observed for rotors **R1**.[19,20,43]

Assessment of E_{RB} for Michael Additions. The rotational barriers showed a clear qualitative correlation with electrophilicity, as reflected in the number of electron-withdrawing groups (EWGs) on the Michael acceptors (Table 1). The unsubstituted control rotor **R1i**, with the weakest unsubstituted alkene electrophile, had the highest rotational barrier (19.8 kcal/mol). Rotors **R1a-e** with one electron-withdrawing group had 1-2 kcal/mol lower barriers (18.8 to 17.6 kcal/mol). Rotors with **R1f-h**

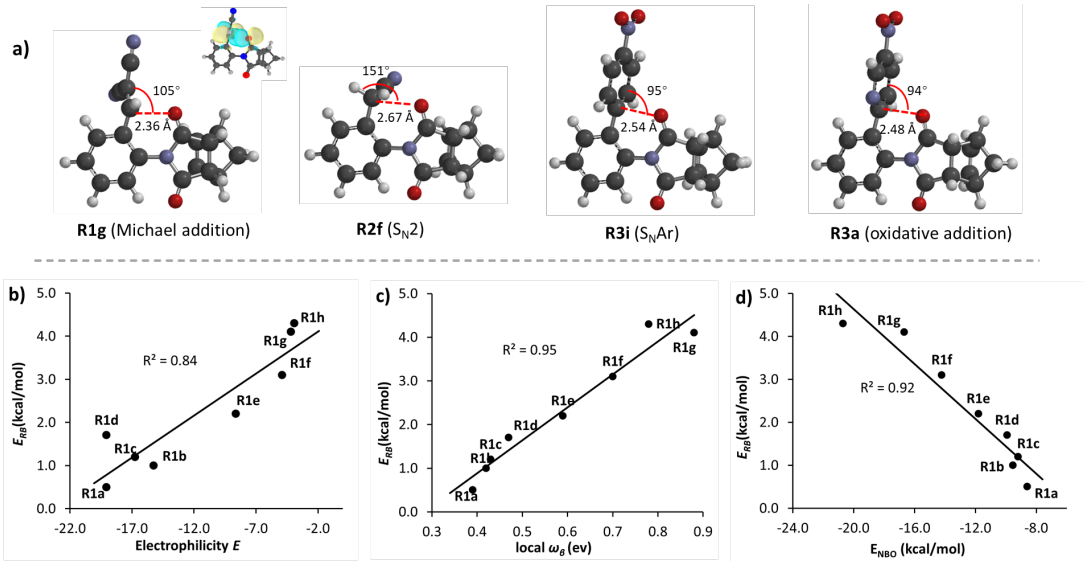

Figure 4. a) Examples of calculated TS structures (B3LYP-D3/6-311G*) of the rotors R1g, R2f, R3i, and R3a, highlighting the similarity of the intramolecular C=O•••electrophile distance and interaction angles with reaction TS that they are mimicking. (inset: NBO second-order perturbation illustrating the oxygen lone-pair → Michael acceptor π* donation in R1g.) b) Correlation plot of E_{RB} for rotors R1a to R1h and the Mayr empirical electrophilic parameter *E* for the corresponding Michael acceptors E1a-h. c) Correlation plot of the measured E_{RB} for rotors R1a-h and the computational electrophilic parameter local ω_β for the corresponding Michael acceptors E1a-h. d) Correlation plot of the measured E_{RB} and the calculated natural bond order (E_{NBO}) energies for the TS nucleophile-electrophile interaction energies.

Table 1. Experimental ΔG‡, E_{RB}, electrophile pyramidalization Θ, and NBO energy (E_{NBO}) parameters for molecular rotors R1a-i.

Rotors	ΔG‡[a]	E_{RB} [b]	*Pyram Θ* [c]	E_{NBO} [d]
R1a	19.3	0.5	6.6	-8.6
R1b	18.8	1.0	6.9	-9.5
R1c	18.6	1.2	6.5	-9.2
R1d	18.1	1.7	6.7	-9.9
R1e	17.6	2.2	7.3	-11.8
R1f	16.7	3.1	8.1	-14.2
R1g	15.7	4.1	8.6	-16.7
R1h	15.5	4.3	12.9	-20.7
R1i	19.8	0.0	4.0	-4.4

[a]Rotational barriers (kcal/mol) measured by EXSY ^{1}H NMR with an error of ± 0.2 kcal/mol. [b]$E_{RB} = \Delta G^{\ddagger}_{(R1i)} - \Delta G^{\ddagger}_{(R1x)}$ where $\Delta G^{\ddagger}_{(R1x)}$ is the rotational barrier of the rotor containing the electrophile of interest. [c]Degree of pyramidalization (°) of the electrophilic carbon in the *ortho*-substituent of rotors **R1** of the electrophilic group. [d]Second-order perturbation theory energy of natural bond orbitals at the ωB97M-V/6-311+G* level of theory for the sum of orbital interactions (kcal/mol) between the C=O oxygen lone pairs and electrophilic carbon of Michael acceptor groups.

with two electron-withdrawing groups had 3-4 kcal/mol lower barriers (16.7 to 15.5 kcal/mol).

Encouraged by the qualitative correlations, we next assessed the ability of E_{RB} to quantitatively predict electrophilicity trends of the Michael acceptors. For the Michael addition electrophiles **E1**, E_{RB} was defined as the difference between the control rotor **R1i** and the rotational barrier of the molecular rotor containing the Michael acceptor of interest. The reason **R1i** was chosen as the control rotor is that its R-group is only an ethylene group without EWGs and thus was the weakest Michael acceptor. For consistency, the ethylene rotor **R1i** was also used as the control for the E_{RB} values for alkyl and aryl electrophiles **E2** and **E3**.

The E_{RB} values for the Michael acceptor electrophiles **E1a-h** ranged from 4.3 kcal/mol for **R1h,** which contains two carboxylic ester EWGs, to 0.0 kcal/mol for the unsubstituted alkene **R1i**. These E_{RB} values were correlated with Mayr's experimental electrophilicity parameter *E* (Figure 4b).[32] For **E1a-d**, the *E* values were reported in the literature.[32] For **E1e-h**, the *E* values were derived from those of their corresponding styrenyl Michael acceptors, which have a phenyl group at the γ-carbon. Mayr *et al.* showed that the influence of the γ-phenyl group is constant for Michael acceptors.[32] Based on this, we estimated the *E* values for **E1e-h** by subtracting the average phenyl contribution (5.33) from the reported *E* values for the γ-analogs. A plot of E_{RB} versus *E* (Figure 4b) showed a good correlation (R^2 = 0.84), demonstrating the ability of E_{RB} to predict electrophilicity trends. This linear correlation also validates the extrapolated *E* values for electrophiles **E1e-h**.

In addition to correlations with Mayr's experimental parameter, a strong correlation (R^2 = 0.95) was also observed (Figure 4c) between E_{RB} and the computational electrophilicity parameter, local electrophilicity index (ω_β), which was calculated at the Michael acceptor carbon atom.[32] The local ω_β parameter, derived from conceptual DFT, reflects only electrostatic and orbital contributions to electrophilicity and does not account for steric effects. The strong agreement between E_{RB} and local ω indicates that E_{RB} effectively captures attractive components of electrophilicity, which is consistent with its expected sensitivity to non-covalent interactions in the bond rotation transition state.

Basis for E_{RB} Trends. We hypothesized that the ability of the rotors to accurately predict electrophilicity trends in the Michael addition series was due, in part, to the formation of attractive electrostatic and orbital interactions in the bond rotation transition states that were analogous to those present in nucleophile–electrophile bond-forming transition states. Further support for this hypothesis was provided by natural bond orbital (NBO) calculations and structural analyses. Second-order perturbation NBO analysis (ωB97M-V/6-311G*) of the rotor transition states confirmed the presence of $n \rightarrow \pi$ interactions between the imide oxygen lone pairs and the electrophilic carbon of the rotor R-groups (see Figure 4a, inset, for **R1g** as a representative example). The stabilization energies ranged from −8.6 to −20.7 kcal/mol (Table 1), values consistent with previously reported lone pair to π interactions.[21,44,45] Importantly, the second-order NBO stabilization energies correlated well with E_{RB} values (Figure 4d, R^2 = 0.92), supporting that the rotor barriers reflect the strength of attractive orbital interactions.

Additional evidence for orbital interactions in the rotors **R1** was provided by analysis of the electrophilic carbon geometries. In the ground-state structures of **R1a–h**, the electrophilic carbon was sp^2 hybridized and planar as expected, with pyramidalization angles (Θ) of 0.3° to 2°(SI). In contrast, in the transition states, the electrophilic γ-carbons were partially pyramidalized, with Θ values of 6.5° to 12.9°, consistent with oxygen lone pair to carbon π orbital interactions.[46] For reference, an ideal tetrahedral geometry would have a Θ angle of 54.75° (Table 1).

One factor that facilitates the attractive through-space TS interactions is the favorable positioning of the nucleophilic and electrophilic groups in the rotor framework. Examination of the transition state structures showed that the imide C=O oxygen and the electrophilic carbon of the Michael acceptor group are positioned at close distances (2.7 to 3.0 Å) with favorable attack angles (95° to 105° relative to the plane of the π-system). These distances and orientations are similar to those observed in early transition states of Michael additions (2.5 to 2.8 Å). However, we should note that the rotor transition states were not designed to directly model the bond formation transition states; rather, they share geometric and structural features that are expected to lead to similar stability trends.

The analyses of the Michael addition transition states suggest that E_{RB} effectively captures the attractive components of electrophilicity, specifically electrostatic and orbital interactions, that dominate reactivity trends in this series. These reactions were selected in part because substituent effects in common Michael acceptors primarily influence electronics rather than sterics, as the electron-withdrawing groups are typically positioned away from the electrophilic carbon. As a result, steric variation across the series is relatively small. To more directly evaluate the steric sensitivity of E_{RB}, we next examined S_N2 reactions, where steric

hindrance at the reactive center plays a major role in controlling reactivity.

S_N2 electrophiles. First, we examined S_N2 reactions to evaluate the applicability of E_{RB} to a new reaction class. S_N2 reactions are particularly sensitive to steric hindrance at the electrophilic center, making them an effective system to assess the steric sensitivity of E_{RB}.[47,48] In addition to their steric sensitivity, S_N2 reactions offered an opportunity to test E_{RB} on electrophiles that are not included in Mayr's electrophilicity database,[49] allowing us to assess its utility for systems lacking established benchmark parameters. First, a new series of rotors **R2** was designed to study the S_N2 reaction (Figure 5a). Unlike the Michael acceptor electrophiles, the S_N2 electrophiles (**E2**) had leaving groups that were removed to provide attachment to the *ortho*-position of the rotors. The electrophilic carbons in the **E2** electrophiles were sp^3 carbons,[50] their electrophilicities were varied by altering their steric and electronic properties through changes in length (**E2a**, **E2b**, **E2c**), branching (**E2d**), electron-withdrawing groups (**E2f** and **E2h**), or adjacent sp^2 groups (**E2e** and **E2h**).

Rotors **R2a-h** were actually previously described in our study of the origins of the benzylic and allylic electrophile effects in S_N2 reactions.[51] The rotational barriers varied from a high of 23.6 kcal/mol for the sterically hindered *iso*-propyl **R2d** to a low of 20.5 kcal/mol for **R2f** with a strong cyano EWG. The E_{RB} values for electrophiles **E2a-h** were calculated based on the difference in rotational barriers of the control rotor **R1i** and rotors **R2a-h** (Table 2). The E_{RB} values for rotors **R2a–h** ranged from a low of -3.8 kcal/mol for **R2c** to a high -0.5 kcal/mol for **R2h**. All values were negative. This is in contrast to the E_{RB} values for the Michael acceptors, which were positive. These negative values are the result of using the ethylene Michael acceptor rotor **R1i** as the control. However, this does not imply that S_N2 electrophiles are weaker than MA electrophiles. Direct comparison is challenging because the S_N2 electrophiles in this study lack their electron-withdrawing leaving groups, which would otherwise enhance the electrophilicity of the carbon center.

In the TS structures, the electronegative imide oxygen formed the closest contact with the first carbon of the electrophilic group, which corresponds to the electrophilic carbon of the S_N2 reaction (Figure 4a). The O•••C distances in **R2a-h** were significantly shorter (2.67–2.74 Å) than the sum of the vdW radii of O and C (3.22 Å). A representative TS geometry is shown in Figure 4a (second structure) for rotor **R2f**, where the O•••C distance measures 2.67 Å. The TS orientation of the electrophilic group was more difficult to assess as the leaving group was removed. The two hydrogens of the tetrahedral carbon adopt an orientation where one points toward the imide oxygen and the other points away from it. If one considers the hydrogen pointing away as the leaving group, then O•••C-H angle is 151°. This attacking angle resembles the backside nucleophile approach of the S_N2 transition state.[52]

The E_{RB} values for **E2** were consistent with the expected qualitative trends for S_N2 reactions, capturing the effects of steric hindrance, conjugation, and electron-withdrawing groups (EWGs). The steric trend is evident in the alkyl series, where the increasing bulk around the electrophilic center decreases electrophilicity. For example, methyl, ethyl, *n*-propyl groups of **R2a**, **R2b**, and **R2c** have similar E_{RB} values (-1.9, -2,2, and -1.9 kcal/mol). However, the bulkier *i*-propyl of **R2d** has a significantly lower E_{RB} value (-3.8 value). Conjugation effects are captured by the rotors, as seen by allyl and benzyl groups of **R2e** and **R2g** having lower E_{RB} values (-1.4 and -1.1 kcal/mol) than their non-conjugated alkyl counterparts. Finally, the trends correctly reflect the influence of EWGs, with the electron-withdrawing CN and keto groups of **R2f** and **R2h** displaying the highest electrophilicities (-0.7 and -0.5 kcal/mol).

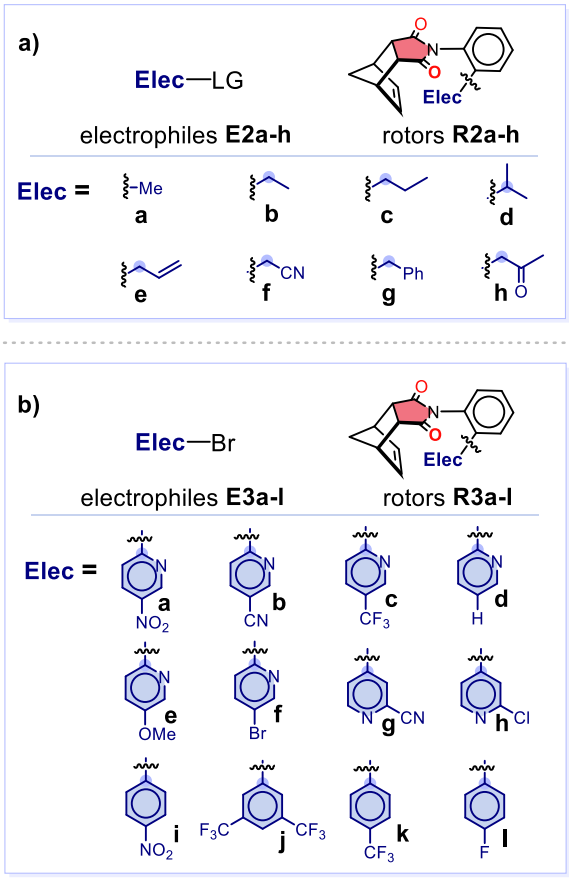

Figure 5. a) Structures of the *N*-phenylsuccinimide rotors **R2** designed to evaluate the utility of E_{RB} for electrophiles **E2** for S_N2 (LG = Cl, Br, I). b) Structures of the *N*-phenylsuccinimide rotors **R3** designed to evaluate the utility of E_{RB} for electrophiles **E3** for S_NAr and Pd(0) oxidative addition reactions. The electrophilic carbons in the electrophiles are highlighted with a blue dot.

The quantitative predictive abilities of the E_{RB} values for the electrophiles **E2** were evaluated by comparing them to a dataset of the experimentally determined relative activation energies for S_N2 reactions ($\Delta\Delta G^{\ddagger}_{SN2}$).[53,54] This experimental data was originally compiled by Streitwieser and reanalyzed by Rablen.[53,54] The $\Delta\Delta G^{\ddagger}_{SN2}$ values represent the average S_N2 reaction rates of electrophiles with different leaving groups (LG = I, Br, Cl) and a variety of nucleophiles (I^-, Br^-, Cl^-, EtO^-, $S_2O_3^{2-}$, Me_3N, Et_3N, quinuclidine, pyridine, $PhNMe_2$, thiourea). A good correlation was observed (R^2 = 0.88) across the range of S_N2 electrophiles (Figure 6a), which demonstrates E_{RB}'s predictive power for S_N2 reactions. The strong correlation between E_{RB} and experimental S_N2 activation barriers further supports the ability of E_{RB} to capture the repulsive sterics as well as the attractive electrostatic and orbital contributions to electrophilicity.

S_NAr electrophiles. Next, the predictive abilities of E_{RB} were tested for the S_NAr reaction, which again has a very different mechanism. The S_NAr reaction involves nucleophilic attack on an aromatic ring, forming an anionic Meisenheimer intermediate or transition state.[55] Like the S_N2 electrophiles, the S_NAr electrophiles (**E3**) were integrated into rotors **R3** without their halide leaving groups. They were attached to the rotor by the bond originally occupied by the leaving group. This positions the electrophilic aryl carbon in contact with the imide carbonyl oxygen in the TS with distances of 2.48 to 2.57Å, which are again shorter than the sum of the VDW radii (3.22 Å). Figure 4a (third structure) shows a representative TS structure for rotor **R3i** with a *p*-nitrophenyl group. The O•••C (aryl plane) angle was close to perpendicular 95°.

Table 2. Experimental $\Delta G^{\ddagger}_{exp}$, E_{RB}, reaction free energy of activation for S_N2 rotors R2.

Rotors	$\Delta G^{\ddagger}$ [a]	E_{RB} [b]	$\Delta\Delta G^{\ddagger}_{SN2}$ [c]	$\Delta\Delta G^{\ddagger}_{SNAr}$ [d]	$\Delta\Delta G^{\ddagger}_{OA}$ [e]
R2a	21.7	-1.9	0	-	-
R2b	22.0	-2.2	2.02	-	-
R2c	21.7	-1.9	2.57	-	-
R2d	23.6	-3.8	4.2	-	-
R2e	21.2	-1.4	-0.16	-	-
R2f	20.5	-0.7	-2.05	-	-
R2g	20.9	-1.1	-0.82	-	-
R2h	20.3[f]	-0.5	-2.14	-	-
R3a	17.4	2.4	-	0.00	0.00
R3b	17.6	2.2	-	1.88	0.08
R3c	18.1	1.7	-	3.01	0.80
R3d	18.6	1.2	-	5.22	3.17
R3e	19.1	0.7	-	7.29	4.51
R3f	18.5	1.3	-	4.20	-
R3g	18.6	1.2	-	1.54	2.11
R3h	19.2	0.6	-	3.01	3.30
R3i	19.3	0.5	-	3.40	3.70
R3j	19.6	0.2	-	5.16	4.33
R3k	20.3	-0.5	-	-	6.28
R3l	20.5	-0.7	-	-	8.27

[a]Rotational barriers (kcal/mol) of rotors **R2** measured by EXSY ^{1}H NMR with an error of ± 0.2 kcal/mol. [b]$E_{RB} = \Delta G^{\ddagger}_{(R1i)} - \Delta G^{\ddagger}_{(Rx)}$ where $\Delta G^{\ddagger}_{(Rx)}$ is the rotational barrier of the rotor containing the electrophile of interest. [c]Relative reaction activation energy of S_N2 reaction in kcal/mol reanalyzed by Rablen.[53] [d]A competition experiment approach is used to determine relative rates of S_NAr under the conditions of Ar-Br, BnOH, *t*BuOK, DMSO, and r.t. The relative activation energies were calculated with respect to the activation energy of 2-bromo-5-nitropyridine in kcal/mol.[28] [e]A competition experiment approach is used to determine relative rates of oxidative addition under the conditions of Ar-Br, $Pd(PCy_3)_2$, THF, and r.t. The relative activation energies were calculated with respect to the activation energy of 2-bromo-5-nitropyridine in kcal/mol.[29] [f]Calculated rotational barrier at B3LYP-D3/6-311G* level of theory.

The electrophilicity of the aryl groups was attenuated by using heterocyclic 2-pyridyl (**R3a-f**) and 4-pyridyl structures (**R3g-h**) as well as phenyl groups with electron withdrawing substituents (**R3i-l**). Rotors **R3a-l** were synthesized as before, and their rotational barriers were measured. The rotational barriers for rotors **R3a-l** ranged from 17.4 kcal/mol (**R3a**) to 20.5 kcal/mol (**R3l**, Table 2). Qualitative analysis of the **R3a-l** rotor barriers matched the expected trends (Table 2). The rotational barriers for phenyl rotors (**R3i-l**) were the highest (19.3 to 20.5 kcal/mol). The heterocyclic 4-pyridyl rotors (**R3g-h**) were the next highest (18.6 to 19.2 kcal/mol). Finally, the 2-pyridyl rotors (**R3a-f**) with the electronegative group closest to the electrophilic arene carbon was the lowest (17.4 to 18.6 kcal/mol).

For a quantitative analysis, the corresponding E_{RB} values were calculated using **R1i** as the control rotor and compared with the experimentally measured relative reaction energies ($\Delta\Delta G^{\ddagger}_{SNAr}$). This data was measured for S_NAr reaction of the corresponding arylbromides of **E3a-l** reacting with benzyl alkoxide (Figure 6b).[42] The E_{RB} values were positive and varied from 0.2 kcal/mol for **R3j** to 2.4 kcal/mol **R3a**. The strong correlations were observed between the **R3** E_{RB} values and $\Delta\Delta G^{\ddagger}_{SNAr,}$ with $R^2 = 0.97$ and 0.93. This demonstrates that the predictive accuracy of our single parameter E_{RB} is similar to recently developed multiparameter models for the S_NAr reaction.[28] Notably, E_{RB} shows two distinct reactivity trends, with the 2-pyridyl halides in one trendline and the 4-pyridyl and phenyl halides in the other. E_{RB} predicts that the 2-pyridyl halides will be more reactive than the 4-pyridyl halides, which is opposite to the general S_NAr reactivity trend.[56] Although there are nucleophiles and reaction conditions that can favor reaction at the 2-pyridyl halides as is predicted by E_{RB}.[57]

Pd-oxidative addition. The utility of E_{RB} was further demonstrated by applying it to a fourth reaction class. Specifically, the E_{RB} values for the aryl halide electrophiles **E3** originally developed for the S_NAr reaction were used to predict the reactivities of Pd-oxidative addition reactions. Not only does E_{RB} accurately predict the reactivities, but it also accurately predicts the relative selectivities of the 2-pyridyl, 4-pyridyl, and substituted arylhalides. Pd-oxidative addition is a key step in many C-C bond forming coupling reactions, including the Suzuki, Heck, and Sonogashira.[58–60] While the Pd oxidative addition reaction is not commonly classified as a nucleophile-electrophile reaction, the reaction involves an electron-rich Pd(0) species oxidatively inserting into a polarized halogen-carbon bond.[61] Notably, the Pd-oxidative addition reaction mechanism has also been observed to have similarities to the S_NAr mechanism.[62]

Paci and Leitch recently measured the relative rates of the Pd-oxidative insertion reaction for a series of substrates that could be used for comparison.[29] Specifically, they measured the free energies of activation for the insertion of $Pd(PCy_3)_2$ for a series of aryl bromides which overlap with the electrophiles used in the S_NAr study (**E3a-e**, **E3g**, **E3h**, **E3i**, and **E3j**). Two additional arylhalide electrophiles, **E3k** and **E3l** were added for this study, requiring synthesis and barrier measurement. The E_{RB} values for **E3** were compared with the experimentally measured relative reaction energies ($\Delta\Delta G^{\ddagger}_{OA}$) for the Pd-oxidative addition reactions.[29] Linear regression analysis yielded an R^2 value of 0.94, indicating a strong correlation (Figure 6c). These findings support the generality of E_{RB}, which extends even to reactions involving metal nucleophiles. Equally impressive is that the aryl electrophiles **E3**, including the 2-pyridyl, 4-pyridyl, and substituted phenyl, all fall on a single trendline. This demonstrates that E_{RB} is accurately predicting the relative reactivities in the Pd-oxidative addition reaction regardless of the arene or substitution pattern.

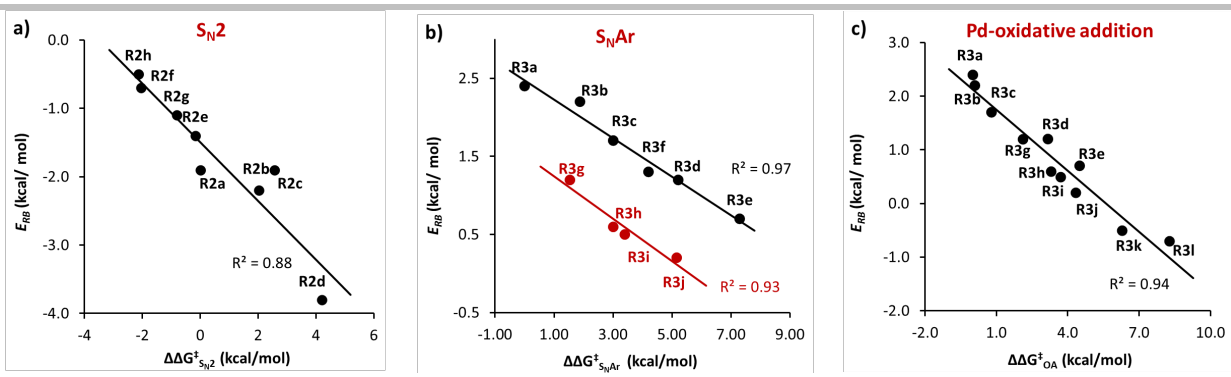

Figure 6. a) Correlation plot of E_{RB} and the activation energies ($\Delta\Delta G^{\ddagger}_{SN2}$) for the corresponding S_N2 substrates.[53] b) Correlation plot of E_{RB} and the activation energies ($\Delta\Delta G^{\ddagger}_{SNAr}$) for the corresponding S_NAr 2-bromopyridines (black line) and 4-bromopyridines/bromobenzenes (red line).[28] c) Correlation plot of E_{RB} and the corresponding Pd(0) oxidative addition activation energies ($\Delta\Delta G^{\ddagger}_{OA}$) of bromobenzenes.[29]

Sonogashira reaction. Finally, we sought to test whether E_{RB} values obtained from DFT calculated rotational barriers could also be used to accurately predict reactivity trends. This approach could be useful for systems that are difficult to synthesize or measure, or for electrophiles for which E_{RB} values have not yet been reported. This expectation was based on the strong agreement between the DFT calculated and experimental barriers for rotors **R1**, **R2**, and **R3**, which were within ±0.6 kcal/mol with an R^2 of 0.89 (see SI). This hypothesis was tested by calculating the E_{RB} parameter for a new set of arylbromide electrophiles **E4a-q**, corresponding to rotors **R4a-q** that were never synthesized. These would be evaluated against the experimental rates (log *k*) reported for the Sonogashira reaction (Figure 7).[63] The ground state and transition state structures for rotors **R4a-q** were calculated at the B3LYP-D3/6-311G* level of theory. The corresponding rotational barriers were used to generate E_{RB} values. In addition, calculations were performed for the rotational barriers of rotors **R3i**, **R3k**, and **R3l**, which had been previously determined experimentally. Their calculated values (19.5, 20.3, 20.8 kcal/mol) were within ±0.2 kcal/mol (RMS error) of the experimental values (19.3, 20.3, 20.5 kcal/mol).

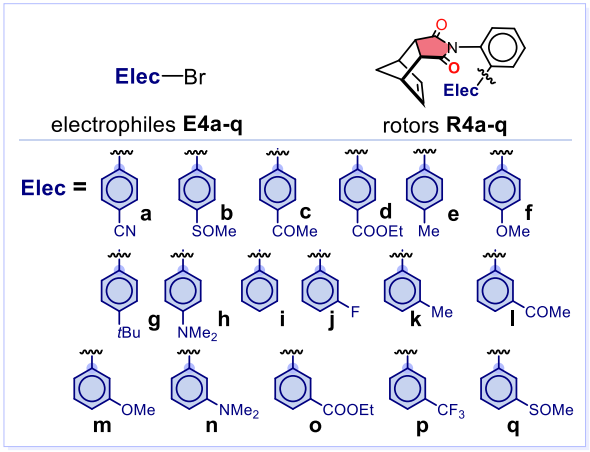

Figure 7. Structures of the *N*-phenylsuccinimide rotors **R4** designed to evaluate the utility of the calculated E_{RB} values for electrophiles **E4a-q** in the Sonogashira reaction. In addition, the calculated E_{RB} values for **E3i**, **E3k**, and **E3l** were used in the analysis.

The calculated E_{RB} values for 20 electrophiles (**R4a-q**, **R3i**, **R3k**, **R3l**) were correlated with the experimentally measured rates Sonogashira reactions of arylbromides with phenylacetylene (HN*i*Pr$_2$, 80 °C, Na_2PdCl_4, CuI, *n*Bu$_3$P·HBF$_4$=4:3:4).[63] A strong correlation (Figure 8a) was observed with an R^2 value of 0.90, which was similar to the accuracy of the experimental E_{RB} values providing support for the utility of the calculated E_{RB} values.

Beyond reactivity predictions, E_{RB} can provide mechanistic insights by probing how attractive and steric interactions influence transition states. This mechanistic utility is evident in the Sonogashira reaction, where the predictive accuracy of E_{RB} varies depending on the rate-determining step of the reaction. This variation was evident in the differing correlations between E_{RB} values and experimental reaction energies under different conditions. To investigate the influence of ligand sterics, we generated correlation plots analogous to Figure 8a for a series of phosphine ligands and recorded the R^2 values for each fit. These R^2 values were then plotted against the cone angle (θ) of the corresponding ligands in Figure 8b.

This analysis revealed a clear trend: smaller ligands gave strong correlations (R^2 > 0.8), while bulky ligands produced poor correlations (R^2 < 0.5). This highlights how E_{RB} can be used to detect changes in mechanisms. The highest predictive accuracy was observed for small phosphine ligands such as *n*Bu$_3$P (Figure 8a). In contrast, bulky ligands gave poor fits between E_{RB} and the experimental log *k* values for these Sonogashira reactions (Figure 8b). The observed shift in correlation with increasing ligand size is consistent with the known dependence of the Sonogashira reaction mechanism on phosphine bulk.[64,65] For less bulky ligands, the reaction typically proceeds through an associative pathway, where the rate-determining step is the insertion of Pd into the aryl halide bond. In contrast, with bulky ligands, ligand dissociation becomes the rate-determining step, reducing the influence of aryl halide electrophilicity on the overall reaction rate.[66] This distinction underscores how E_{RB} effectively predicts reactivity under specific conditions by revealing the influence of ligand sterics on mechanistic pathways.

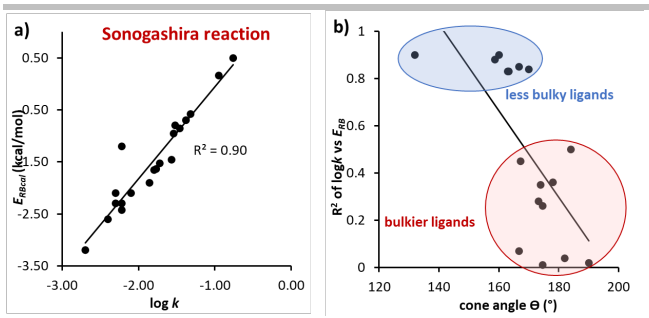

Figure 8. a) Correlation plot between calculated E_{RB} and the experimental *log k* for Sonogashira reactions of 20 aryl bromides with phenylacetylene under the condition of HN*i*Pr$_2$, 80 °C, Na_2PdCl_4, CuI, *n*$Bu_3P{\cdot}HBF_4$=4:3:4. b) Correlation plot between the R^2 of *log k* (measured under the condition of different ligands) versus E_{RB}, and the corresponding cone angle of the ligand.

When applying E_{RB} to predict electrophilicity trends, several considerations should be kept in mind. Although each correlation in this study is based on a relatively small panel of eight to ten substrates, those panels were deliberately chosen to bracket the full electronic and steric range of their reaction class, and the resulting fits (R^2 = 0.84–0.97) reproduce long-established reactivity orderings. The use of a consistent nucleophilic probe (the imide C=O lone pair) across all electrophiles ensures internal consistency and allows comparisons of a broader range of electrophiles. However, caution is warranted when comparing E_{RB} values across different reaction classes. One reason is the absence of leaving groups in the rotor-bound electrophiles, which can significantly affect reactivity in real systems, particularly for reactions like S_N2 and S_NAr where leaving group effects are important. Although the constrained geometry of the rotor framework helps maintain well-defined distances and orientations between the nucleophile and electrophile that enhance the reproducibility of the measured trends, it does not compensate for missing structural features like leaving groups. This limitation is reflected in occasional deviations within a class of electrophiles, such as the difference observed between 2- and 4-pyridyl bromides (**E3**) in the S_NAr reactions.

A final distinguishing feature of E_{RB} is its foundation in kinetic measurements that directly probe transition state interactions. In contrast to traditional electrophilicity parameters, such as Hammett σ constants or the Gutmann–Beckett Lewis acidity scale, which are derived from ground-state thermodynamic equilibria, E_{RB} values are obtained from rate measurements that reflect the stabilization of transition states. This distinction is particularly relevant for reactions governed by transition state effects. In the rotor system, the interacting groups are constrained to distances shorter than the van der Waals radii during bond rotation, approximating the short atom-to-atom separations observed in bond forming transition states. This structural feature may enable E_{RB} to more effectively capture the energetic contributions that influence reactivity along the reaction coordinate.

CONCLUSION

In conclusion, this study introduces E_{RB}, a new empirical electrophilicity parameter derived from the rotational barriers of *N*-phenylimide molecular rotors containing electrophilic groups. E_{RB} provides a useful and accessible means of assessing electrophilicity, offering improved predictive accuracy and mechanistic insight. Its utility was demonstrated by strong correlations with established experimental and computational electrophilicity parameters for a series of Michael acceptors, as well as with activation energies for S_N2, S_NAr, Pd-oxidative addition, and Sonogashira reactions. These results demonstrate that E_{RB} effectively captures electrophilicity trends across a broad range of mechanistically distinct reactions by incorporating both attractive (electrostatic and orbital) interactions and steric effects. This ability to account for both types of reactivity factors supports the broader utility of E_{RB} as a general electrophilicity parameter. Modeling studies of the bond rotation transition states indicate that E_{RB} reflects intramolecular interactions between the electrophilic group and the lone pairs on the succinimide oxygens. In addition to enabling prediction, E_{RB} offers mechanistic insight into transition state stabilization in both S_N2 and cross-coupling reactions. The ability to account for steric effects and to be estimated computationally further supports its potential as a versatile tool for organic synthesis, drug discovery, and materials design.

Supporting Information

Crystallographic data for structures 1a and 3c have been deposited at the Cambridge Crystallographic Data Centre, CCDC numbers 2380188 and 2390532. The authors have cited additional references within the Supporting Information.

Conflict of Interest

The authors declare no conflict of interest.

Acknowledgements

This work was supported by the National Science Foundation Grant CHE 2304777.

Keywords: Molecular Rotors; Electrophilicity; Rotational Barrier; Structure-Reactivity; Physical Organic Chemistry

[1] D. Wondrousch, A. Böhme, D. Thaens, N. Ost, G. Schüürmann, *J. Phys. Chem. Lett.* **2010**, *1*, 1605–1610.
[2] H. Jangra, Q. Chen, E. Fuks, I. Zenz, P. Mayer, A. R. Ofial, H. Zipse, H. Mayr, *J. Am. Chem. Soc.* **2018**, *140*, 16758–16772.
[3] D. T. Ahneman, J. G. Estrada, S. Lin, S. D. Dreher, A. G. Doyle, *Science* **2018**, *360*, 186–190.
[4] O. Engkvist, P.-O. Norrby, N. Selmi, Y. Lam, Z. Peng, E. C. Sherer, W. Amberg, T. Erhard, L. A. Smyth, *Drug Discov. Today* **2018**, *23*, 1203–1218.
[5] E. N. Muratov, J. Bajorath, R. P. Sheridan, I. V. Tetko, D. Filimonov, V. Poroikov, T. I. Oprea, I. I. Baskin, A. Varnek, A. Roitberg, O. Isayev, S. Curtalolo, D. Fourches, Y. Cohen, A. Aspuru-Guzik, D. A. Winkler,

D. Agrafiotis, A. Cherkasov, A. Tropsha, *Chem. Soc. Rev.* **2020**, *49*, 3525–3564.
[6] L. C. Gallegos, G. Luchini, P. C. St. John, S. Kim, R. S. Paton, *Acc. Chem. Res.* **2021**, *54*, 827–836.
[7] M. Vahl, J. Proppe, *Phys. Chem. Chem. Phys.* **2023**, *25*, 2717–2728.
[8] Corwin. Hansch, A. Leo, R. W. Taft, *Chem. Rev.* **1991**, *91*, 165–195.
[9] L. P. Hammett, *Chem. Rev.* **1935**, *17*, 125–136.
[10] H. H. Jaffé, *Chem. Rev.* **1953**, *53*, 191–261.
[11] U. Mayer, V. Gutmann, W. Gerger, *Monatshefte Für Chem.* **1975**, *106*, 1235–1257.
[12] D. A. Kutateladze, D. A. Strassfeld, E. N. Jacobsen, *J. Am. Chem. Soc.* **2020**, *142*, 6951–6956.
[13] S. J. Zuend, E. N. Jacobsen, *J. Am. Chem. Soc.* **2009**, *131*, 15358–15374.
[14] C. B. Santiago, J.-Y. Guo, M. S. Sigman, *Chem. Sci.* **2018**, *9*, 2398–2412.
[15] C. B. Santiago, A. Milo, M. S. Sigman, *J. Am. Chem. Soc.* **2016**, *138*, 13424–13430.
[16] R. Ruzziconi, S. Spizzichino, L. Lunazzi, A. Mazzanti, M. Schlosser, *Chem. – Eur. J.* **2009**, *15*, 2645–2652.
[17] A. Mazzanti, L. Lunazzi, R. Ruzziconi, S. Spizzichino, M. Schlosser, *Chem. – Eur. J.* **2010**, *16*, 9186–9192.
[18] L. Lunazzi, M. Mancinelli, A. Mazzanti, S. Lepri, R. Ruzziconi, M. Schlosser, *Org. Biomol. Chem.* **2012**, *10*, 1847.
[19] E. C. Vik, P. Li, J. M. Maier, D. O. Madukwe, V. A. Rassolov, P. J. Pellechia, E. Masson, K. D. Shimizu, *Chem. Sci.* **2020**, *11*, 7487–7494.
[20] B. Lin, H. Liu, I. Karki, E. C. Vik, M. D. Smith, P. J. Pellechia, K. D. Shimizu, *Angew. Chem. Int. Ed.* **2023**, *62*, e202304960.
[21] E. C. Vik, P. Li, P. J. Pellechia, K. D. Shimizu, *J. Am. Chem. Soc.* **2019**, *141*, 16579–16583.
[22] B. Lin, H. Liu, H. M. Scott, I. Karki, E. C. Vik, D. O. Madukwe, P. J. Pellechia, K. D. Shimizu, *Chem. – Eur. J.* **2024**, *30*, e202402011.
[23] E. C. Vik, P. Li, D. O. Madukwe, I. Karki, G. S. Tibbetts, K. D. Shimizu, *Org. Lett.* **2021**, *23*, 8179–8182.
[24] S. Staniland, R. W. Adams, J. J. W. McDouall, I. Maffucci, A. Contini, D. M. Grainger, N. J. Turner, J. Clayden, *Angew. Chem. Int. Ed.* **2016**, *55*, 10755–10759.
[25] H. Mayr, M. Patz, *Angew. Chem. Int. Ed. Engl.* **1994**, *33*, 938–957.
[26] R. Lucius, R. Loos, H. Mayr, *Angew. Chem. Int. Ed.* **2002**, *41*, 91–95.
[27] R. Appel, H. Mayr, *J. Am. Chem. Soc.* **2011**, *133*, 8240–8251.
[28] J. Lu, I. Paci, D. C. Leitch, *Chem. Sci.* **2022**, *13*, 12681–12695.
[29] J. Lu, S. Donnecke, I. Paci, D. C. Leitch, *Chem. Sci.* **2022**, *13*, 3477–3488.
[30] P. K. Chattaraj, U. Sarkar, D. R. Roy, *Chem. Rev.* **2006**, *106*, 2065–2091.
[31] R. G. Parr, L. V. Szentpály, S. Liu, *J. Am. Chem. Soc.* **1999**, *121*, 1922–1924.
[32] D. S. Allgäuer, H. Jangra, H. Asahara, Z. Li, Q. Chen, H. Zipse, A. R. Ofial, H. Mayr, *J. Am. Chem. Soc.* **2017**, *139*, 13318–13329.
[33] Q. Chen, P. Mayer, H. Mayr, *Angew. Chem. Int. Ed.* **2016**, *55*, 12664–12667.
[34] N. F. Fine Nathel, L. A. Morrill, H. Mayr, N. K. Garg, *J. Am. Chem. Soc.* **2016**, *138*, 10402–10405.
[35] Z. Li, R. J. Mayer, A. R. Ofial, H. Mayr, *J. Am. Chem. Soc.* **2020**, *142*, 8383–8402.
[36] X. Guo, H. Mayr, *J. Am. Chem. Soc.* **2014**, *136*, 11499–11512.
[37] P. Li, E. C. Vik, K. D. Shimizu, *Acc. Chem. Res.* **2020**, *53*, 2705–2714.
[38] J.-M. Tian, Y.-H. Yuan, Y.-Y. Xie, S.-Y. Zhang, W.-Q. Ma, F.-M. Zhang, S.-H. Wang, X.-M. Zhang, Y.-Q. Tu, *Org. Lett.* **2017**, *19*, 6618–6621.
[39] D. Rani, V. Gulati, M. Guleria, S. P. Singh, J. Agarwal, *J. Mol. Struct.* **2022**, *1265*, 133341.
[40] W. R. Carroll, P. Pellechia, K. D. Shimizu, *Org. Lett.* **2008**, *10*, 3547–3550.
[41] W. I. Nicholson, J. L. Howard, G. Magri, A. C. Seastram, A. Khan, R. R. A. Bolt, L. C. Morrill, E. Richards, D. L. Browne, *Angew. Chem. Int. Ed.* **2021**, *60*, 23128–23133.
[42] "Molecular Orbitals and Organic Chemical Reactions, Reference Edition | Wiley," can be found under https://www.wiley.com/en-ae/Molecular+Orbitals+and+Organic+Chemical+Reactions%2C+Reference+Edition-p-9781119964674, **n.d.**
[43] B. Lin, I. Karki, P. J. Pellechia, K. D. Shimizu, *Chem. Commun.* **2022**, *58*, 5869–5872.
[44] H. Zheng, H. Ye, X. Yu, L. You, *J. Am. Chem. Soc.* **2019**, *141*, 8825–8833.
[45] K. B. Muchowska, D. J. Pascoe, S. Borsley, I. V. Smolyar, I. K. Mati, C. Adam, G. S. Nichol, K. B. Ling, S. L. Cockroft, *Angew. Chem.* **2020**, *132*, 14710–14716.
[46] R. W. Newberry, R. T. Raines, *Acc. Chem. Res.* **2017**, *50*, 1838–1846.
[47] S. Liu, H. Hu, L. G. Pedersen, *J. Phys. Chem. A* **2010**, *114*, 5913–5918.
[48] M. Gallegos, A. Costales, Á. Martín Pendás, *J. Comput. Chem.* **2022**, *43*, 785–795.
[49] "Mayr's Database Of Reactivity Parameters - Start page," can be found under https://www.cup.lmu.de/oc/mayr/reaktionsdatenbank/, **n.d.**
[50] J. Xie, W. L. Hase, *Science* **2016**, *352*, 32–33.
[51] B. Lin, H. Liu, X. Huang, H. M. Scott, P. J. Pellechia, K. D. Shimizu, *Angew. Chem. Int. Ed.* **n.d.**, *n/a*, e202505483.
[52] G. Vayner, K. N. Houk, W. L. Jorgensen, J. I. Brauman, *J. Am. Chem. Soc.* **2004**, *126*, 9054–9058.
[53] P. R. Rablen, B. D. McLarney, B. J. Karlow, J. E. Schneider, *J. Org. Chem.* **2014**, *79*, 867–879.
[54] A. Streitwieser, *Solvolytic Displacement Reactions*, McGraw-Hill, **1962**.
[55] S. Rohrbach, A. J. Smith, J. H. Pang, D. L. Poole, T. Tuttle, S. Chiba, J. A. Murphy, *Angew. Chem. Int. Ed.* **2019**, *58*, 16368–16388.
[56] M. Schlosser, T. Rausis, C. Bobbio, *Org. Lett.* **2005**, *7*, 127–129.
[57] S. G. Ruggeri, B. C. Vanderplas, B. G. Anderson, R. Breitenbach, F. J. Urban, I. Stewart A. Morgan, G. R. Young, *Org. Process Res. Dev.* **2008**, *12*, 411–413.
[58] R. Martin, S. L. Buchwald, *Acc. Chem. Res.* **2008**, *41*, 1461–1473.
[59] C. Amatore, A. Jutand, *Acc. Chem. Res.* **2000**, *33*, 314–321.
[60] H. Doucet, J.-C. Hierso, *Angew. Chem. Int. Ed.* **2007**, *46*, 834–871.
[61] J. Lu, H. Celuszak, I. Paci, D. C. Leitch, *Chem. – Eur. J.* **2024**, *30*, e202402282.
[62] M. J. Kania, A. Reyes, S. R. Neufeldt, *J. Am. Chem. Soc.* **2024**, *146*, 19249–19260.
[63] M. R. an der Heiden, H. Plenio, S. Immel, E. Burello, G. Rothenberg, H. C. J. Hoefsloot, *Chem. – Eur. J.* **2008**, *14*, 2857–2866.
[64] M. Schilz, H. Plenio, *J. Org. Chem.* **2012**, *77*, 2798–2807.
[65] M. an der Heiden, H. Plenio, *Chem. Commun.* **2007**, 972–974.
[66] E. Galardon, S. Ramdeehul, J. M. Brown, A. Cowley, K. K. (Mimi) Hii, A. Jutand, *Angew. Chem.* **2002**, *114*, 1838–1841.

Entry for the Table of Contents

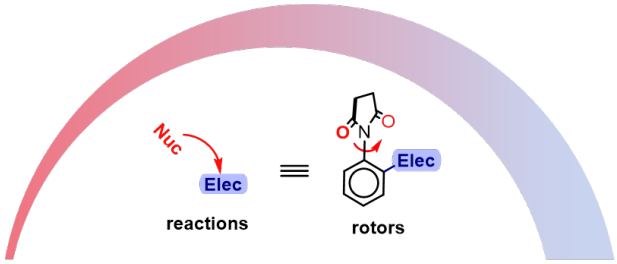

Stronger Elec = Faster reaction rate = Faster rotation speed

A new empirical parameter, E_{RB}, quantifies electrophilicity from rotational barriers of *N*-phenylimide molecular rotors. E_{RB} predicts reactivity trends in Michael additions, S_N2, S_NAr, Pd-oxidative addition, and Sonogashira reactions by capturing both attractive and repulsive transition state interactions.